Journal of Molecular Liquids 388 (2023) 122716

Contents lists available at ScienceDirect

Journal of Molecular Liquids

journal homepage: www.elsevier.com/locate/molliq

State and role of water confined in cement and composites modified with metakaolin and additives

Vanda Papp [a,b,*], Róbert Janovics [b,c], Tamás Péter Kertész [a], Zoltán Nemes [b], Tamás Fodor [d], István Bányai [a], Mónika Kéri [a,*]

[a] University of Debrecen, Department of Physical Chemistry, Egyetem tér 1, Debrecen H-4032, Hungary
[b] Isotoptech Zrt., Debrecen H-4026, Hungary
[c] International Radiocarbon AMS Competence and Training Center INTERACT, Institute for Nuclear Research, Bem tér 18/C, Debrecen H-4026, Hungary
[d] Institute for Nuclear Research, H-4026, Debrecen, Bem tér 18/C, Hungary

ARTICLE INFO

Keywords:
Water mobility
Restricted diffusion
Cement hydration
Cement
Metakaolin
NMR relaxometry
NMR cryoporometry

ABSTRACT

Cement as a porous material contains pores and cracks on the whole nanoscale forming an interconnected pore structure. Its interaction with water during the rehydration of cement plays a key role in every application, such as in nuclear waste treatment, where cement binders are commonly used for conditioning liquid radioactive waste. In the prediction of the long-term disposal the knowledge of water mobility and distribution in the formed porous cement matrix is essential.

In this study we systematically investigate the effects of metakaolin and several components of the liquid phase (complexing agents, model ions, boric acid, etc.) on the hydrated solid structure by various nuclear magnetic resonance (NMR) methods. The novelty lies in the complex use of such non-conventional techniques that separately provide only partial information of the cement structure; however, the gained results complete each other to offer a new approach in the structural study under several conditions. Water mobility is deduced from NMR T_2 relaxation distributions and D_2O-H_2O exchange diffusion measurements, and the conclusion on structural properties is supported by the macropore structure revealed from NMR cryoporometry and SEM (scanning electron microscopy) images, as well as by following the formation of pores and water domains in the curing process with NMR relaxometry. The results confirm that metakaolin was built into the CSH (calcium silicate hydrate) gel region without altering its mesoporous structure, however, it significantly decreased the capillary pore size and the diffusion coefficient of water. Complexing agent concentration between 2 and 20 g/l and the presence of model ions did not cause significant structural changes, while the rehydration decreased the size of capillary pores due to swelling.

1. Introduction

The most common conditioning method for low- and intermediate-level nuclear waste is cementation, during which radioactive components are immobilized in a solid, cement-based matrix.[1–3] The basic material of the technology is Portland cement, a mixture of inorganic crystalline materials (clinkers). During the hydration of cement crystalline portlandite ($Ca(OH)_2$) and amorphous CSH as major phases (calcium silicate hydrate, $1.7CaO{\cdot}SiO_2{\cdot}xH_2O$), while aluminoferrite trisulphate ($[Ca_3(Al,Fe)(OH)_6{\cdot}12H_2O]X_3{\cdot}H_2O$) (X = sulphate), aluminoferrite monosulphate ($[Ca_2(Al,Fe)(OH)_6]X{\cdot}H_2O$), hydrogarnet ($3CaO{\cdot}Al_2O_3{\cdot}6H_2O$) as well as hydrotalcite ($Mg_6Al_2(CO_3){\cdot}(OH)_{16}{\cdot}4(H_2O)$ as minor phases are formed. Among these, the CSH phase is the most significant due to its large surface area which helps the immobilization of radionuclides through several chemical changes (precipitation, adsorption, ion exchange, etc.).[3–7].

Although the hydration of Portland cement is an extensively researched topic, there are several points of this process which are still not certain. Based on calorimetric and conductivity measurements, solution phase analysis, X-ray diffraction and many other techniques the

* Corresponding authors at: University of Debrecen, Department of Physical Chemistry, Egyetem tér 1, Debrecen H-4032, Hungary (V. Papp).
E-mail addresses: papp.vanda@science.unideb.hu (V. Papp), janovicsrobert@isotoptech.hu (R. Janovics), tamaskertesz07@gmail.com (T. Péter Kertész), nemeszoltan@isotoptech.hu (Z. Nemes), fodor.tamas@atomki.mta.hu (T. Fodor), banyai.istvan@science.unideb.hu (I. Bányai), keri.monika@science.unideb.hu (M. Kéri).

https://doi.org/10.1016/j.molliq.2023.122716
Received 15 May 2023; Received in revised form 26 July 2023; Accepted 28 July 2023
Available online 29 July 2023

hydration process can be divided into five stages.[8,9] The formation of the CSH, which is the product of the hydration of alite (Ca_3SiO_5) and belite (Ca_2SiO_4) anhydrous phases, dominates the hydration process. In the initial period (stage I), the wetting of the cement grains, the fast dissolution of clinker phases and the formation of ettringite ($Ca_6Al_2(SO_4)_3(OH)_{12}{\cdot}26H_2O$) takes place. Afterwards, in the induction period (stage II), the reaction slows down, which can be explained by two hypotheses: the protective membrane and the dissolution control theories.[8,9] After this stage of reduced reactivity, the main product (CSH) precipitates in the acceleration period (stage III), which is followed by the declaration (stage IV) and slow hydration periods (stage V). In the last stages the aluminate containing phases, like ettringite and sulphoaluminates, are formed. During the hydration of cement a hardened porous structure is formed from a saturated colloidal dispersion through complex chemical reactions. At the moment of mixing anhydrous cement and water, the system can be considered as a coarse dispersed system, where the micron-sized cement particles are dispersed in the aqueous phase. This increasingly turns into a colloid-like system, where the dissolution of the silicate and aluminate phases from the surface of the cement takes place and a supersaturated $Ca(OH)_2$ solution is formed. The rigid gel structure of the CSH gel is formed during the aggregation of several 5–10 nm sized globular units containing defective CSH sheets.[10,11].

In the hardened cement structure water domains of different mobility are present. According to the Power-Brownyard model water in a solidified cement structure can be grouped as chemically bound, non-vaporizable water (the crystal and interlayer water of cement hydration products) and vaporizable, pore-filling water (including water in capillary and air pores, and physically bound water in gel pores).[12] In place of the evaporated water, a heterogeneous porous solid structure remains, with pores of different sizes. On the basis of the Feldman-Sereda model and experimental pore-size determinations these are: intra CSH sheet pores (d = 0.5–1.8 nm), inter CSH gel pores (d = 2–10 nm), capillary pores (d = 20/50 nm-1 μm) and air pores (μm to mm size), as later illustrated in Fig. 3a [13–18].

In order to use cement for waste conditioning, it is important to improve its leaching properties. On the one hand, this can be achieved by the application of silicate-based additives, for instance, already 5% kaolinite in the cemented waste can significantly decrease the leaching rate of Cs and Co.[19] Nowadays, an artificial silicate, metakaolin is often used as an additive, since it can improve the cement structure due to its pozzolanic and hydraulic properties, furthermore, it is able to neutralize the acidic components of the radioactive waste.[20,21] On the other hand, complexing agents, like citric acid and oxalic acid, are used for the management of the liquid waste.[2] These additives and the formed complexes can chemically interact with the cement hydration products, and thus modify the surface properties and the structure of the formed cement composite.[22].

The characterization of the structure and aqueous behavior of cement composites is essential since the porosity ultimately affects other properties of the material during the possible applications and the long-term storage. Nuclear magnetic resonance (NMR) methods are outstanding in studying the interaction of porous materials with water, as well as for the characterization of water mobility and the hydrated structure, which we recently demonstrated for various porous materials.[23–25].

In NMR relaxometry we follow the return of the excited magnetic spins of the hydrogen nuclei (protons) in water molecules to the equilibrium state. This process can be described with relaxation time constants (T_1 or T_2). T_2 characterizes the rate of the relaxation in the transverse plane. The transverse relaxation time constant depends on the mobility of the protons, thus the water types of different mobility in the sample can be distinguished. Since the intensity of the NMR peak is proportional to the water amount of the given type, the ratio of bound and more mobile water (*e.g.* in pores) can be determined.[26–28] The observed transverse relaxation rate constant ($1/T_2$) can be expressed by the weighted average of the relaxation rate of the mobile water in the bulk-like ($1/T_{2bulk}$) and the bound water in the surface region ($1/T_{2s}$) provided fast molecular exchange between these water types:

$$\frac{1}{T_2} = \frac{V_s}{V}\frac{1}{T_{2s}} + \frac{V_{bulk}}{V}\frac{1}{T_{2bulk}} \tag{1}$$

where V is the total volume of the measurable water, V_s and V_{bulk} are the volumes of the surface water and the bulk water respectively. T_2 is the observed apparent transverse relaxation time, while T_{2bulk} and T_{2s} are the characteristic relaxation time constants of water molecules in the bulk-like and surface regions respectively.

Furthermore, the pore size of saturated pores in the nm size range can be calculated according to Eq. (2), if the surface relaxivity (ξ) is known.[29].

$$\frac{1}{T_2} = \xi\frac{S_p}{V_p} + \frac{1}{T_{2bulk}} \tag{2}$$

where S_p is the surface and V_p is the volume of the pores.

Low-field (LF) NMR relaxometry techniques are more accessible, cheaper and less sensitive to magnetic impurities compared to high-field NMR, and thus are effective in the characterization of cement materials, both their hydration process and the hardened state.[30,31] In hydrated cement several water domains can be distinguished by their T_2 relaxation time constants, which are in good agreement with the above-mentioned pore-filling water types in cement.[14–16,31,32] Similarly, the mobility of water within the system changes during the hydration of cement, thus this process can also be observed by NMR relaxometry. Pop et al. followed the process of hydration in the case of cement samples, during which they found a significant change in the measured T_2 transverse relaxation time constants for ~ 20 h after mixing with water.[33] This time interval was divided into 5 periods based on the changes seen in the relaxation time constants and were ordered to the different stages of cement hydration.[33] Faure and Rodts studied the change of the longitudinal relaxation time (T_1) of water during the hydration process and identified two liquid domains as the bulk water and the gel water surrounding the cement grains. The change of T_1 over time showed the five- stage behavior characteristic for cement hydration.[34] The curing process of cement is strongly influenced by several parameters such as the water-cement ratio, the composition of cement and the type of additives. Rusu et al. investigated the effect of calcium nitrate, a hydration accelerator additive, on the early hydration of a white cement paste. It was found that the induction period shortened in the presence of calcium nitrate, proving that the effect of additives can also be detected by following the curing process of binders by NMR.[9].

Another technique which can be successfully applied in the structure characterization of porous materials is NMR cryoporometry.[35,36] Liquids in nano-sized confinements show different melting-freezing phase transition temperature than in bulk. The observed melting- and freezing point depressions can be converted into pore sizes according to the modified Gibbs-Thomson equation:

$$\Delta T_{m/f} = T_{m/f} - T_0 = -\frac{nK_c}{r_p} \tag{3}$$

where $T_{m/f}$ is the melting and freezing point of the liquid in the porous system, T_0 is the phase transition temperature of the bulk liquid, n is a factor characteristic for the pore geometry, K_c is the cryoporometric constant of the liquid (determined by the V_m, molar volume, γ_{SL}, solid–liquid interfacial tension, ΔH, heat of melting and the T_0 of the liquid), while r_p is the radius of the pore.[35] Valckenborg *et al.* completed their relaxometric studies with cryoporometry experiments and revealed three pore types in mortar.[18] Clay minerals can also be investigated by NMR cryoporometry, however, due to their layer-like structure only freezing-point depression can be expected to detect. In the case of cured modified metakaolin, pores between ca. 2–40 nm were observed and assigned to three different parts of the zeolite structure.[37].

With the help of NMR diffusometry, the self-diffusion (Brown - movement) coefficient of water can be determined, the value of which significantly depends on the confining effect of the pore structure. The restricted diffusion processes provide valuable information about the size and permeability of the pores in the range of 5–100 μm. Diffusion is conventionally measured using gradient pulses in the so-called stimulated spin-echo sequence (PGSTE) by NMR. However, in the case of samples containing magnetic inhomogeneities the T_1 and T_2 relaxation processes of confined water are significantly accelerated, therefore this sequence is not suitable for investigating diffusion processes. For testing such systems the so-called H_2O–D_2O exchange diffusion technique can be applicable.[38] The basis of the method is to place the sample, saturated with light water (H_2O), into heavy water (D_2O) and follow the decreasing intensity of the proton signal within the sample due to the H_2O–D_2O exchange process. An important criterion of the test is the strictly cylindrical geometry of the sample and the high heavy to light water ratio (α).[38] During the evaluation of the primary data series, the exponential curves can be fitted with a mathematical model derived by J. Crank suitable for describing diffusion from a cylinder.[39] In this model, diffusion processes in an infinite cylinder (C_{cyl}) and in a plane sheet (C_{ps}) are included, as the product of two exponentials:

$$C^* = \frac{M(t) - M(t=\infty)}{M(t=0) - M(t=\infty)} = C_{ps}C_{cyl} \tag{4}$$

$$C_{ps} = \sum_{n=0}^{\infty} \frac{2\alpha(1+\alpha)}{1+\alpha+\alpha^2 p_n^2} exp\left(-D_p p_n^2 \frac{t}{l^2}\right) \tag{5}$$

$$C_{cyl} = \sum_{n=0}^{\infty} \frac{4\alpha(1+\alpha)}{4+4\alpha+\alpha^2 p_n^2} exp\left(-D_p p_n^2 \frac{t}{r^2}\right) \tag{6}$$

where C^* is the change in the concentration of light water, M is the intensity of the measured signal, α is the volume ratio of heavy to light water, p_n is the square root of the error function, D_p is the diffusion coefficient of water, t is the duration of the measurement, r and l are the radius and length of the cylinder, respectively.[38,39].

The aim of this study was to thoroughly describe the interactions between water and the porous structure of cement-based materials by various NMR methods, and compare the effects of metakaolin and other additives on them. For this reason, the formation of the cement structure was followed in the early state of the hydration process by NMR relaxometry. The hardened cement and its composite with metakaolin were characterized by SEM images, measuring the size of pores in the structure by NMR cryoporometry, the T_2 transverse relaxation times and the self- diffusion properties of water molecules in the pore system. Furthermore, we studied how a basic model solution, the concentration of complexing agents and the presence of model ions, as well as the rehydration time influence the pore structure and water mobility by T_2 relaxometry.

2. Material and methods

2.1. Preparation of cement samples

First Portland cement and metakaolin containing cement composites were prepared. Portland cement (CEM I 42.5 N) was mixed with deionized water in 0.48 water-cement (w/c) ratio, and cured for 30 days. Metakaolin (KM60) consisted of 50–55% SiO_2, min. 40% Al_2O_3, max. 1.45% Fe_2O_3, 0.05–0.5 % CaO, 0.20–0.45 % MgO and max. 1.5% $K_2O + Na_2O$. The cement composite with 0.5 water-cement ratio were prepared from Portland cement (80%) with 20% metakaolin content (KM60). The liquid phase was deionized water on the one hand, and a model solution of 0.44 mol HNO_3 (65% solution, VWR, a.r.), 0.44 mol KOH (Molar, a.r.), 3.28 mol NaOH (Molar a.r.) and 3.08 mol boric acid (Molar, a.r.) for 1 L solution, on the other hand, simulating the conditions of application.

To study the effect of complexing agents and model ions, two sample series were prepared. The first series of cement composite samples contained complexing agents, citric acid (VWR, Reag. Ph. Eur.), oxalic acid (Molar, a.r.spec.), Na_2-EDTA (Molar, puriss), in 1:1:1 mass ratio, in different concentrations (2, 20, 200 g/l). For the second series inactive metal salts, modeling radioactive isotopes, (0.34 mmol **Nb**$(NO_3)_5$, 2.42 mmol **Cs**NO_3, 5.48 mmol **Ni**$(CH_3COO)_2{\cdot}4H_2O$, 2.22 mmol **Nd** $(NO_3)_3{\cdot}6H_2O$, 2.52 mmol K**I**, 90.6 mmol K**Cl**, 0.16 mmol NH_4**Re**O_4 for 1 L solution) were added to the liquid phase beside the complexing agents. The cement samples were cured for 30 days under high (100%) humidity, and then stored in wet or dry (relative humidity around 50–60%) medium to model different storage conditions.

2.2. Scanning electron microscopy imagining (SEM)

The surface morphology of the Portland cement and 20% metakaolin containing cement composite samples was investigated with a dual beam scanning electron microscopy type Thermo Fisher Scientific-Scios 2 (FIB-SEM, Waltham, MA, USA) operated at low accelerating voltage (2 keV). Applying such low energy and short working distance (2 mm) allows us to study surface morphology of insulating samples without coating it with gold layer. The advantage of using a low accelerating voltage (1–2 keV) is that the secondary electrons generated near the surface can easily escape and in this way, we can increase its yield. The increased yield increases the probability of collecting the electrons needed for imaging, thereby providing the opportunity to examine insulating samples without application of gold coating, which may modify the surface morphology. In order to detect signals with such a small working distance, special detector strategies are required. The microscope used is equipped with a so-called in-lens detection system that has the ability to separate and collect secondary electrons, back scattered electrons, or a mixture of both types of signals.

2.3. NMR relaxometry measurements

For NMR relaxometry experiments the samples were broken in a mortar and then larger pieces suitable for the NMR tube (10 mm) were soaked in deionized water (MilliQ) for three days. Measurements were performed on a 20 MHz NMR instrument (Minispec Bruker mq20) at room temperature (25 °C) using the CPMG (Carr-Purcell-Meiboom-Gill) pulse sequence.[40,41] 0.08 ms echo time and 0.5–1 s relaxation delay were applied. The obtained exponential curves were inverse Laplace transformed in the MERA (Multi Exponential Relaxation Analysis) program running under Matlab software.[42] This data evaluation method results in a T_2 distribution with the most characteristic relaxation times in the maxima. These values were further confirmed by multi-exponential fitting based on the least squares' method with the OriginPro © program.

The curing process of pure cement and the 20 % metakaolin containing cement composite was also followed by NMR relaxometry with the same experimental setup. Portland cement was mixed with distilled water in 0.48 water-cement (w/c) ratio, while w/c = 0.5 was used for the 20 % metakaolin containing composite. The cement pastes were immediately poured into an NMR tube (10 mm), and the T_2 relaxation decays were recorded using the CPMG (Carr-Purcell-Meiboom-Gill) pulse sequence for 48 h. The echo time was 0.08 ms with a 2 s relaxation delay. The process of primary data evaluation is described above.

2.4. NMR cryoporometry measurements

The crushed cement samples were studied in cyclohexane as test liquid. Samples were prepared in 5 mm glass NMR tubes 3 days before the measurement, after the saturation the excess amount of liquid was removed. NMR cryoporometry measurements were performed on a Bruker Avance II 360 MHz NMR instrument with a QNP direct probe. The probe-head was cooled with dried air by a BCU-05 cooling unit. A spin-echo sequence was used for the measurement where the optimal

echo time was 8–10 ms for cyclohexane. Temperature calibration was performed by measuring the temperature dependent chemical shifts of neat methanol.[43] During the experiments the frozen samples were melted first and then freezing and melting measurements were carried out in the temperature range appropriate for the used liquid medium. At each temperature a proton spectrum was recorded, which was then transformed with MestreNova9.0 software. The integrated intensity changes of the proton signals as a function of temperature gave the system-specific freezing and melting curves. Using the modified Gibbs-Thomson equation (Eq. (3) the pore size was calculated[35], and the pore size distribution was obtained by numerical derivation. A model-free cryoporometry constant (K_c = 96 nm K for cyclohexane) determined by Petrov and Furo[35] was used for the calculations.

2.5. Diffusion experiments

The diffusion of water was studied in the pure Portland cement (w/c ~ 0.46) and in the cement- metakaolin composite (20% metakaolin, w/c ~ 0.5), using cylindrical sample geometry with a length of 21–22 mm and a diameter of 7 mm. The cylinders were soaked in distilled water for several days, then placed in at least tenfold (α = 10) excess of heavy water (D_2O, VWR) immediately before the measurement. The pD was previously adjusted to the pH of the soaking water (pD ~ 13.8), using cc. NaOD. The NMR measurement was performed on a 20 MHz NMR instrument (Minispec Bruker mq20) at room temperature (25 °C). During the experiment, the intensity of water protons within the sample was recorded as a function of time by FID sequence. To obtain a high signal to noise ratio 512 scans were used, the waiting time between each scan was set to 0.5 s, as a relaxation filter. This way only the change in the amount of water located inside the cement samples was detected, considering the contribution of the external liquid to the signal (~18%). The exchange process between H_2O– D_2O was followed every 5 min for 6 days in case of pure cement and 9 days in case of metakaolin containing composite. The resulting intensity values were corrected, normalized, and then plotted as a function of the observation time. The obtained curves were fitted with the mathematical model derived by J. Crank (Eq. 4–6).

3. Results and discussion

3.1. Effect of metakaolin

3.1.1. Hydration process and structure formation

By following the hydration process of cement-based binders, the evolution of the confined water can be visualized during the formation of the porous system. Water is the reaction partner of the clinker phases in this process, which results in the change of its mobility and quality due to the formed hydration products. The hydration process of Portland cement and a metakaolin containing cement composite was followed with NMR relaxometry for two days, during which the transversal relaxation time constants of water (T_2) were determined. Three water domains with different mobility characterized the cement binders. The longest T_2 relaxation time (T_2 ~ 40–15 ms) values were uncertain at the beginning of the curing process but reached a stable value after two days. This domain can be assigned to the water filling the formed capillary pores based on T_2 values measured by Bede *et al.* and Liu *et al.*

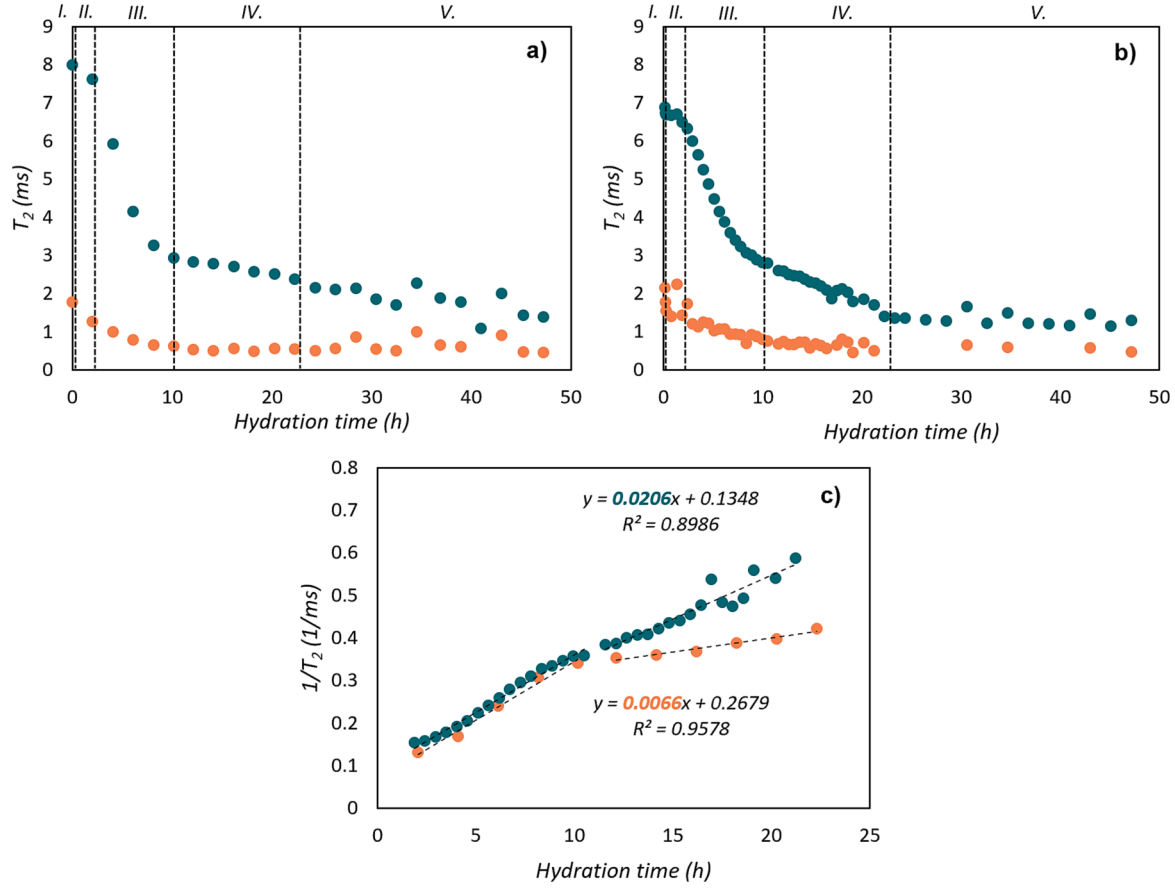

Fig. 1. T_2 relaxation time values over time for a) Portland cement and b) for 20% metakaolin containing cement composite during the hydration process. Different colors show water in the intra CSH sheet (orange) and inter CSH gel pores (blue). The 5 stages of the hydration period are numbered and indicated with dashed lines. c) The reciprocal representations of T_2 assigned to the CSH gel pores for Portland cement (orange) and the metakaolin containing composite (blue) show the CSH formation rate difference between the samples.

[16,32]. The change of the T_2 relaxation time constants in time for the other two domains are shown in Fig. 1. The water domain with $T_2 = 8–2$ ms can be assigned to water forming and filling the inter CSH gel pores. The T_2 value of this type of water changes most significantly in parallel with the formation of the structure, so this is the most informative domain for further conclusions. The shortest T_2 relaxation time ($T_2 \sim 2 – 0.4$ ms) also changes slightly during the hydration and can be categorized as water in the intra CSH sheet pores.

The change of the T_2 relaxation times of the presented two water domains as a function of hydration time can be divided into 5 stages (Fig. 1), as explained in the introduction. The first, very short, initial period (*I.*) could be measured only in the presence of metakaolin (Fig. 1b), where the T_2 relaxation time decreased drastically due to the rapid formation of ettringite. In the induction period (*II.*) the T_2 times were constant for at least two hours, which can be explained by the inhibited formation of CSH gel. After the dissolution of appropriate amount of calcium-silicate, the formation of calcium-silicate-hydrate (CSH) gel starts in the acceleration period (*III.*). From the hydration reaction of alite and belite, portlandite is released, which can react with the excess aluminosilicate source, like metakaolin. The change of the T_2 relaxation times of the two material is quite similar until the declaration period (*IV.*), where the aluminate containing phases form. At the same time in the *IV.* period, the established alkaline environment enables the dissolution of the excess aluminosilicate source and its transformation into CSH gel during its reaction with portlandite. Due to the larger amount of CSH, the formation of the solid structure is faster in the case of the metakaolin containing cement composite. The reciprocal representations of T_2 relaxation times assigned to the CSH gel pores make the reaction rate difference between the two processes more visible (Fig. 1c). During the *III.* period (2–10 h) the slope of the two curves is identical, as the reaction between water and the clinker phases starts similarly. As the metakaolin dissolves in the alkaline system and forms extra CSH, the two curves diverge, and an order of magnitude difference between the slope values appears. Finally, in the last slow hydration period (*V.*) the T_2 relaxation times characteristic of the water in the pores of the hardened cement were observed.

The effect of added metakaolin can be detected at other stages of the hydration process as well. In the initial and induction periods, the T_2 relaxation time of water in the CSH gel pores starts to decrease from lower value in the metakaolin containing sample, and the T_2 relaxation time values of the less mobile water in CSH are scattering. According to Eq. (2)., lower T_2 relaxation time constant refers to water in smaller confinements or stronger interaction between the liquid and the solid surface (higher surface relaxivity).

3.1.2. Structure of dry cement-based binders

The dry structure of the formed ordinary Portland cement and the metakaolin containing composite was compared by scanning electron microscopy analysis (Fig. 2). The main hydration products, plate-like shaped portlandite and spike-like calcium-silicate hydrate can be found in both binders. In the case of pure cement needle-like units are present which can be assigned to ettringite.[8,44,45] This hydrate phase is not visible in the metakaolin containing sample probably due to the large-scale formation of CSH gel. Metakaolin, as a synthetic pozzolan, reacts with lime, released from the hydration reaction of alite and belite, through the Si_4^+ ions at the end of the tetrahedrons to form CSH gel as described in Section 3.1.1.[7] Therefore, the structure of the hardened composite is more compact and less permeable compared to pure cement.

3.1.3. Structure of the hardened binders in water

3.1.3.1. Portland cement. Water in different types of pores in saturated porous materials can be distinguished by their transverse relaxation time constants. In pure cement (see Fig. 3a and b), the relaxation of bound water in the smaller intra CSH layer pores and inter CSH gel pores is faster (short T_2 relaxation time), while the more mobile water molecules filling the larger capillary or air pores show longer relaxation times. From the T_2 distribution curves also the ratio of these water domains can be determined, which strongly depends on the water-cement ratio used during the preparation and indicates the porosity of the hardened cement.[16,46].

Fig. 3b shows the T_2 distribution curve of Portland cement, resulting from the inverse Laplace transformation of the measured exponential decay of proton signal intensity. From the maxima of the curve four different relaxation domains and the relating water types can be distinguished. Their quantitative contributions (Fig. 3b, expressed in %) are in good agreement with the pore ratio found in the literature regarding the applied $\sim$ 0.48 water-cement ratio.[46] Thus, we identified the water types and the corresponding pore types as follows: intra CSH sheet water ($T_2 = 0.5–0.6$ ms), inter CSH gel water ($T_2 = 1–4$ ms) and capillary water ($T_2 = 20–25$ ms). This is also confirmed with comparable ratios and T_2 relaxation times published by Bede *et al.* and Liu *et al.*[16,32].

3.1.3.2. Cement composite containing metakaolin. After the identification of water types in the pure material, we prepared a cement composite adding metakaolin in 20% to the Portland cement (80%). In order to model the circumstances of the possible application in radioactive waste conditioning, a basic model solution (containing HNO_3, KOH, boric acid and NaOH) was used as liquid phase (see details in the Experimental). As shown in Fig. 3c after 3 days soaking the T_2 distribution of water in this sample is similar to that of the pure cement sample in Fig. 3b. It means that the added metakaolin takes part in the formation of the cement hydration product (CSH region) through the pozzolanic reactions known from the literature.[8,20,21] A difference can be observed only in the case of inter CSH gel pores, the distribution of which broadens and incorporates the two maxima of the pure cement.

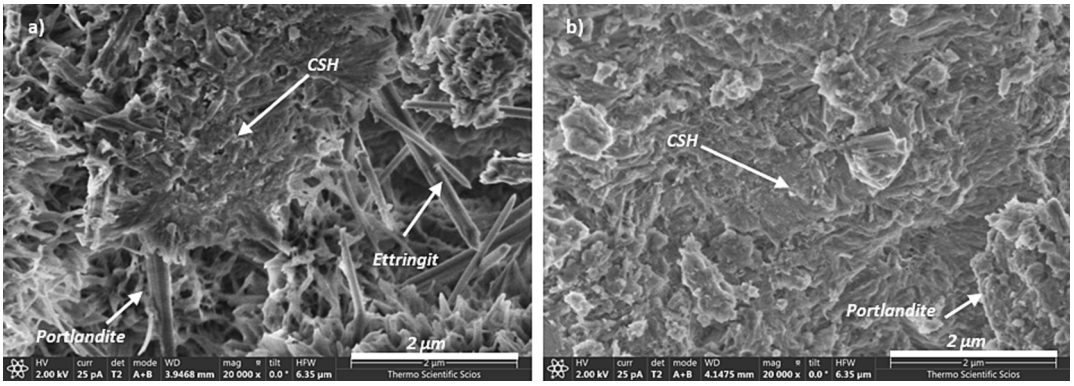

Fig. 2. Scanning electron microscopy images of a) Portland cement and b) the composite containing 20% metakaolin with the characteristic hydration products.

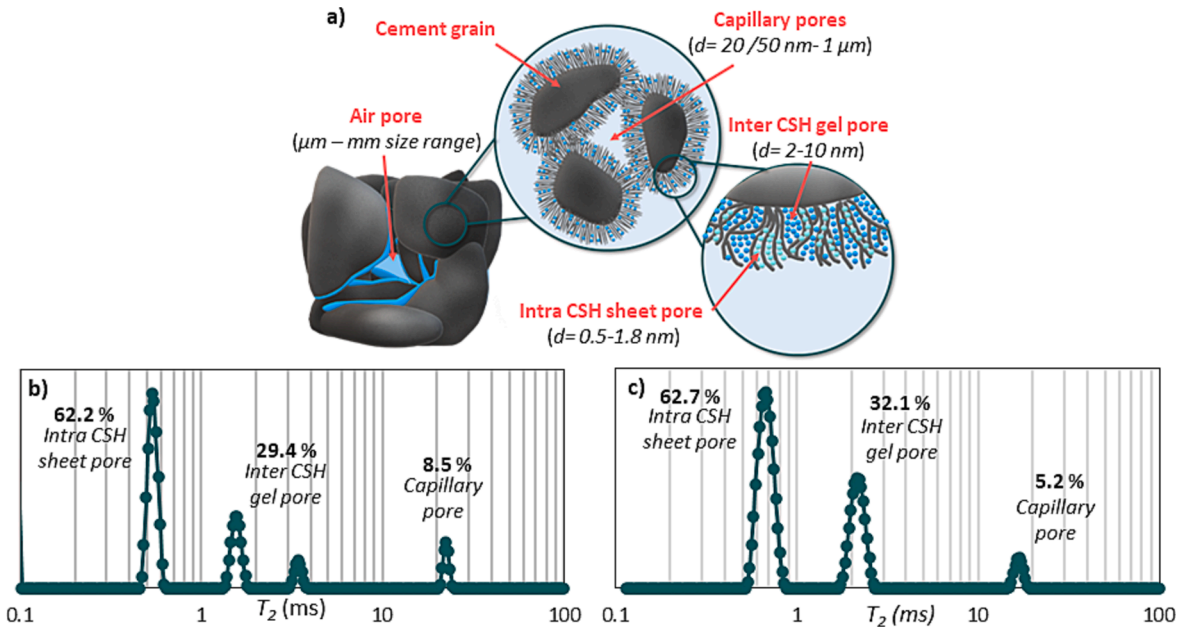

Fig. 3. a) Schematic pore structure of cement and T_2 relaxation time distribution in b) hardened Portland cement and c) 20% metakaolin containing cement composite with the identified pore types and their ratios (%).

Other slight differences between the two T_2 distributions can be explained with the higher w/c ratio of the cement composite due to the presence of metakaolin.

3.1.4. Pore size analysis of the hydrated binders

For the two samples, Portland cement and cement composite with metakaolin, the size determination of the pores was carried out by NMR cryoporometry on the one hand, and by the conversion of the relaxometric results to size by Eq. (2) on the other hand.

In the first case the geometry and the size of the compartments inside and between the solid grains of the two samples were determined by NMR cryoporometry. The pore system of the samples was saturated with cyclohexane since in aqueous medium the formed fast-relaxing cement hydration product disables the measurement with high-field NMR. The intensity changes of the obtained proton spectra as a function of the temperature gave the melting and freezing curves, shown in Fig. 4.

The observed freezing-point depressions and the lack of melting-point depressions indicate slit-like pore geometry in both cases, which is also supported by the SEM images, where the amorphous structure of various compounds showed no regular spherical or cylindrical pore structure on the micrometer scale. The size of these pores, i.e., the distance of the slit walls, was determined using Eq. (3) with a geometry factor $n = 1$ for slit-like pores. The calculated r_p is the half-distance between the slit walls, from which the whole distance is $d = 2r$. [35,47].

The insets in Fig. 4. show the pore size distributions of the two samples resulting from the freezing curves. In pure cement the freezing point depression was ~ 0.2 K, while in the cement-metakaolin composite it was ~ 0.7 K (Fig. 4a and b). The obtained pore size distributions range from 200 nm to 1600 nm for pure cement with an approximate maximum of ~ 800 nm, and 20–550 nm with a characteristic slit distance of 200–300 nm for the cement composite. We have to note, that these pore sizes are close to the upper detection limit of the NMR cryoporometry technique; however, the observed freezing-point depressions and thus the pore-size distributions show significant differences between the samples. The observed large pore size in pure cement and the cement composite can be mainly attributed to the capillary pores (see Fig. 3a.). Smaller CSH sheet and gel pores could not be detected by NMR cryoporometry because of the fast relaxation of the liquid inside. In the case of pure cement, the distribution is shifted to larger size values (~μm) which can be explained by the microcracks

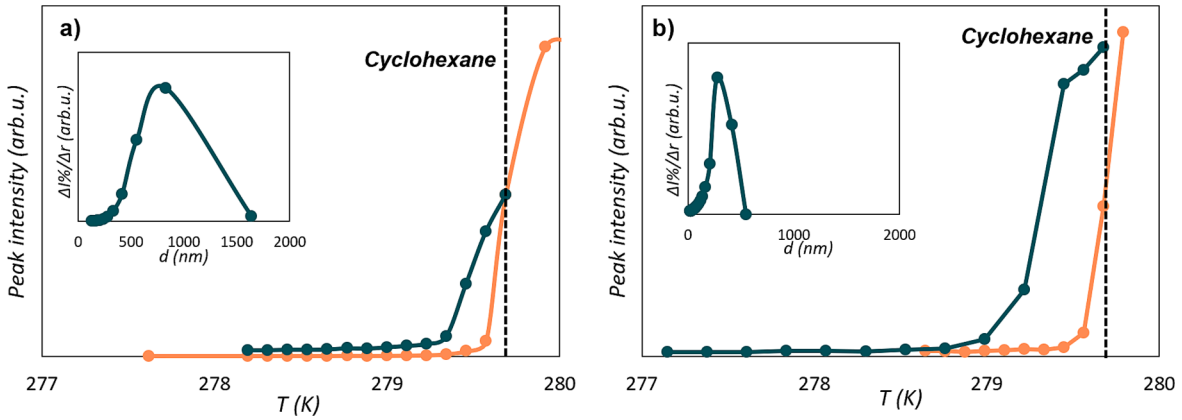

Fig. 4. Melting and freezing curves of Portland cement (a) and 20% metakaolin containing cement composite (b) and the calculated pore size distribution curves (inset). Different colors show the melting (orange) and freezing (blue) curves. The dashed lines stand for the bulk transition temperatures (T_0), while the solid lines are guide for the eye.

formed during the storage. For the cement composite containing metakaolin, the decrease in the pore size and the absence of μm sized pores can be owned to the improving effect of metakaolin.[20].

In the second case, the T_2 transverse relaxation time constants were converted into pore sizes based on Eq. (2). For the calculations the knowledge of surface relaxivity (ξ) is required, which has a substance-specific value depending on the thickness of the surface monolayer of adsorbed water (λ) and its T_2 relaxation time constant (T_{2s}, surface relaxation time):

$$\xi = \frac{\lambda}{T_{2s}} \tag{7}$$

The surface relaxivity of water in the CSH of cement materials is determined in several ways in the literature and thus ranges from 0.9 nm/ms to 3.73 nm/ms.[18,48–50] For the pore size calculations we applied 1.88 nm/ms, calculated from $\lambda = 0.3$ nm, and $T_{2s} = 0.16$ ms measured by Zhou *et al.*[48] Based on the observations in the cryoporometry measurements for larger pores, and on literature evidences of the CSH pores regarded as planar pores or mentioned with layered structure, slit-like geometry was used in the pore-size calculations, thus S_p/V_p is equal to $2/d$ in Eq. (2).[10,51,52] The pore size distributions of the two materials are shown in Fig. 5. As opposed to cryoporometry this way we can get information about the size of the smaller compartments of the structure as well, like the CSH sheet, gel and capillary pores. For the cement and cement composite samples the pore size values are in good agreement with the ones from literature[13–16,31], also shown in Fig. 3, confirming our identification of the water domains in the previous section: intra CSH sheet pores d≈2 nm, inter CSH gel pores d≈6-15 nm and capillary pores with d≈60-90 nm. Significant difference in the pore sizes of these nano-sized confinements cannot be observed.

3.1.5. *Diffusion of water in cement-based binders*

The rate of water diffusion in cement binders is a key-question from the application point of view both as a building material and a binder for liquid-phase waste. However, its experimental determination comes up against difficulties, since the diffusion of water can be quite restricted in the compact cement structure. Furthermore, the use of PGSE NMR is also impossible due to the fact, that the great majority of water relaxes too fast ($T_2 < 5$ ms, see Fig. 3b, c) to detect its diffusion. As a solution, the self-diffusion coefficients of water in the cement and cement-metakaolin composite samples were determined using a special H_2O-D_2O exchange diffusion technique.[38] During the measurement, only H_2O protons inside the cement samples were detected with the help of a relaxation filter, meaning a short (0.5 s) relaxation delay after each scan, which eliminates the long-relaxing bulk water component from the measured signal. The intensity of the measured signal exponentially decreases over time because of the exchange process of water from the whole pore structure with heavy water surrounding the cement sample (Fig. 6a). Comparing the exponential curves of pure cement and the metakaolin containing cement sample, a significant difference can be observed (Fig. 6b). In the case of pure cement, the water signal intensity decreased to 17% of the initial value in two days (see dashed line in Fig. 6b), which was stable for the rest of the measurement. In contrast, the signal intensity in the metakaolin containing sample decreased only to 59% in two days, and reached 34% at the end of the experiment. Fitting the exponential curves with the aforementioned model (Eq. 4–6), the characteristic diffusion coefficients were determined with a maximum fitting error of 10%. The primary data was best fitted as a product of 3 exponential sums. All the three determined diffusion coefficients were much lower than the value assigned to free water ($D = 2.3 \times 10^{-9}$ m^2/s), referring to strongly restricted diffusion of water in the samples. The slowest diffusion process can be assigned to the restricted movement of water in the swollen CSH gel, where the derived diffusion coefficients were $D = 3.1 \times 10^{-12}$ m^2/s for pure cement and $D = 8.2 \times 10^{-12}$ m^2/s for the metakaolin containing one. Comparable results were observed by Fleury et al. using the same method.[53] Capillary, and air pores, due to their larger size, allow higher water mobility, thus the other two diffusion coefficients in pure cement were assigned to these pores with $D = 2.4 \times 10^{-10}$ m^2/s and $D = 9.6 \times 10^{-10}$ m^2/s, which are still far below that of bulk water and typical values for cementitious materials.[38] With the addition of metakaolin to cement, the change in the pore structure, compactness and permeability of the binder were clearly visible form the results of NMR relaxometry, cryoporometry and the SEM images. Due to this structural change the diffusion of water is more restricted, which results in a slower diffusion process of $D = 2.3$–2.4×10^{-11} m^2/s.

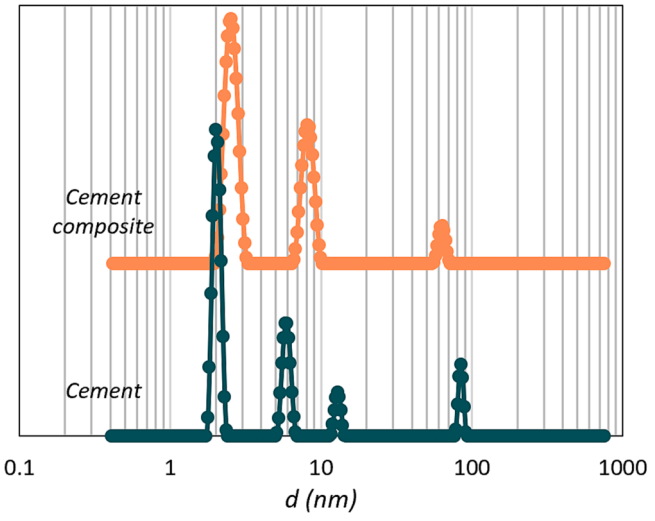

Fig. 5. Pore size distributions of Portland cement and the 20% metakaolin containing cement composite obtained from NMR relaxometry.

3.2. *Effect of possible application conditions*

As it was confirmed, the addition of metakaolin to Portland cement results in a more compact and less permeable pore structure, and various NMR techniques, especially relaxometry, are definitely applicable for the characterization. Consequently, we measured T_2 relaxation time distributions to study the effect of several possible application conditions on the structure of the metakaolin-containing cement composites and the mobility of water therein.

3.2.1. *Time of rehydration*

In order to model the possible rehydration process of dry cement binders during waste storage, we measured the T_2 relaxation of water in the cement composite sample containing metakaolin and model solution for 18 days. The dried samples were immersed in water and the signal of the bulk water was filtered out through relaxation selection, thus the T_2 of the structure filling water was detected.

The measured T_2 distribution, as shown in Fig. 7, does not change significantly until 12 days. The T_2 time constants (0.5–0.6 ms and 1.5–2 ms) and their ratios are similar as evidence of the stable structure of the bound water containing CSH region. It means that water absorbs immediately in these segments after the immersion. The T_2 relaxation time constants attributed to the more mobile inter CSH gel (5–12 ms) and capillary pores (60–120 ms) show slight shift during the rehydration process, which can be explained by the exchange of water molecules in these domains.

After 18 days the distribution broadens, the first two domains merge between $T_2 = 0.5$–2 ms. This can be a result of accelerated exchange between these sites, which is interpreted as the domain of the chemically bound water in the intra CSH is incorporated into the smaller inter CSH gel pores through their swelling (see Fig. 7). The swollen growing hydrated gel region reduces the mobility of water in the larger pores and

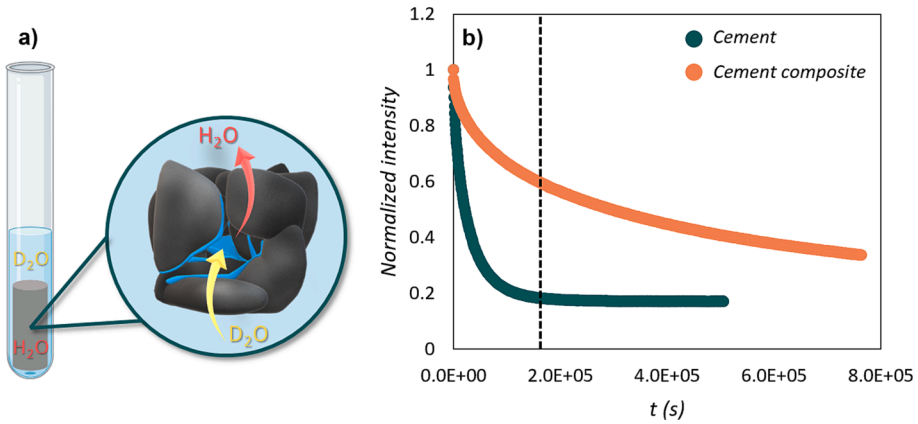

Fig. 6. a) Schematic picture of the H_2O-D_2O exchange diffusion technique representing the diffusion of water from the whole cement structure and b) the measured intensity of the proton signal over time in Portland cement (blue) and the 20% metakaolin containing composite (orange). The dashed line marks the point of comparison at two days.

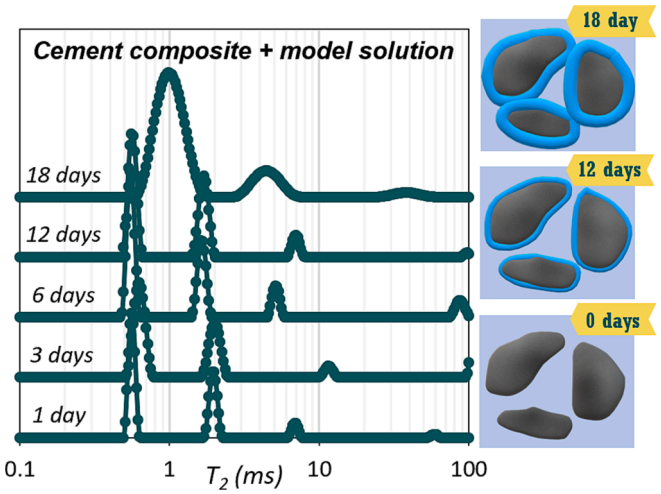

Fig. 7. Change in the T_2 relaxation time distributions of water with the soaking time in the rehydrated cement sample, and the supposed scheme of rehydration.

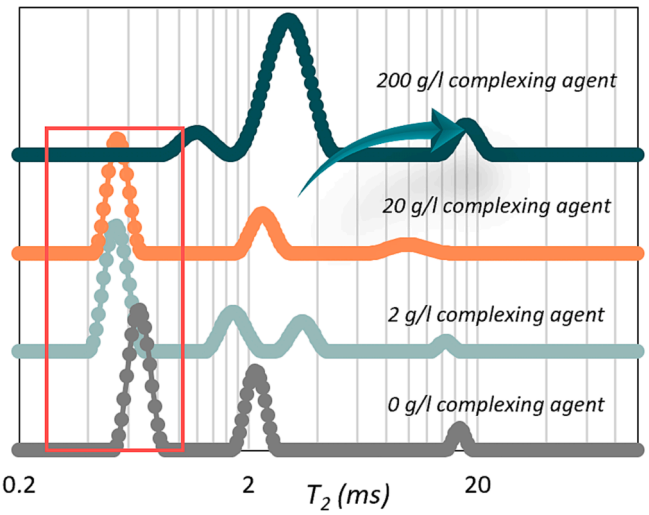

Fig. 8. T_2 relaxation time distributions of water in the hydrated cement samples prepared with model solution and 2, 20 and 200 g/l complexing agent concentration (the arrow highlights the observed shift).

capillaries, which can be observed from the decrease of T_2 and the broadened distributions of the other two domains.

3.2.2. Effect of the complexing agent concentration

Cement composites were prepared with metakaolin, model solution (HNO_3, KOH, boric acid and NaOH), and complexing agents (citric acid, oxalic acid and Na_2-EDTA) in several concentrations, the effect of which on the structural properties of the cement composite was investigated by NMR relaxometry.

Fig. 8 shows that the position and relative amount of the most bound intra CSH type of water do not change significantly in the presence of complexing agents, compared to the pure cement sample. At 20 g/l concentration the T_2 relaxation distribution of the capillary water broadens, suggesting these water domains become somewhat more mobile, and the exchange between them increases.

At 200 g/l complexing agent concentration, the distributions widen and shift significantly (arrow in Fig. 8). The ratio of the intra CSH sheet pores and the inter CSH gel pores interchanges. This change was observed in the macroscopic properties as well, the structure became looser and frangible, which makes the sample unsuitable for the targeted application.

3.2.3. Effect of model ions

A series of cement composites was prepared in the presence of ions modeling the radioactive isotopes. After curing these samples were kept wet in exsiccator under stable humidity.

Changes in relaxation properties are demonstrated by the comparison of the samples with same complexing agent concentration from the 1. and 2. series (the concentration of 200 g/l is not studied further due to the observed radical change in the pore structure). For samples containing model ions, the relaxation domains of water types shifted to a shorter relaxation time range, but the ratios remain unchanged (arrow in Fig. 9). This can be explained on the one hand by the acceleration effect of the added paramagnetic ions on the relaxation rate. On the other hand, the CSH region is capable of ion absorption[1], thus the decreasing relaxation times may be caused by the astringent effect of the added alkali metal ions, but further studies are needed to clarify this.

4. Conclusions

The hydrated structure of cement composites and the mobility of water in the pore system were investigated under the effect of metakaolin, and other additives related to the application by nuclear magnetic methods. These methods reveal new aspects in the characterization of these porous materials and bring much closer to the conditions of applications. For the accurate determination of the effect of metakaolin

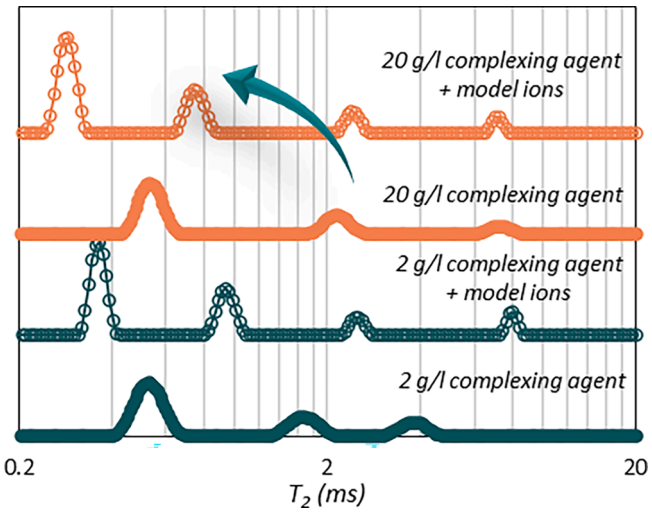

Fig. 9. Effect of model ions on the T_2 relaxation properties of water in cement composites (the arrow highlights the observed shift).

on the cement structure, the hydration process of the binders and the hardened structure were characterized first. Over the hydration process the formation of the solid structure is faster in the case of the metakaolin containing cement composite, due to the precipitation of larger amount of CSH. Metakaolin is built into the CSH gel structure of the formed cement composite and did not alter the nanostructure of the CSH region. However, it significantly decreased the size of the large capillary pores, confirming the expected structural improvement. The more compact structure hindered the diffusion of water within the system, which was inferred from the magnitude change of the determined diffusion coefficients.

We studied the effects of some conditions under the circumstances of the possible application of cement composites as binders of radioactive waste. Through the rehydration of dry cement samples, the swelling of the CSH gel and the shrinking of the capillary pores were observed. Clearly visible differences were found between the cement matrices as a function of the complexing agent concentration. The concentration range between 2 and 20 g/l can be proposed for the immobilization process without any structural change of the binder. The model ions of radioactive compounds might be absorbed in the CSH region, but did not cause significant structural change.

We demonstrated that NMR techniques can be effectively applied in the structural analysis of hydrated cement materials and the characterization of water mobility in the solid matrices, thus these methods can contribute to the optimization and development of proper binders for the final disposal of radioactive waste. Furthermore, the NMR methods reveal the structural reasons for the in-situ behavior of the binders, thus effectively support the standard leaching experiments, widely applied for porous solids in waste immobilization.

CRediT authorship contribution statement

Vanda Papp: Investigation, Data curation, Writing – original draft. **Róbert Janovics:** Conceptualization, Project administration. **Tamás Péter Kertész:** Investigation. **Zoltán Nemes:** Investigation. **Tamás Fodor:** Investigation. **István Bányai:** Writing – review & editing. **Mónika Kéri:** Investigation, Writing – original draft, Conceptualization.

Declaration of Competing Interest

The authors declare that they have no known competing financial interests or personal relationships that could have appeared to influence the work reported in this paper.

Data availability

Data will be made available on request.

Acknowledgement

We are grateful to Dávid Nyul for his technical contribution to the NMR spectroscopic measurements. The research was supported by the KDP-2021 program of the Ministry for Innovation and Technology from the source of the National Research, Development and Innovation Fund [RH/322-2/2022]. The research was also supported by the National Research, Development and Innovation Office – NKFIH [PD 135169, K 131989] and was carried out within the framework of the RHK contract. The SEM measurements were supported by the project 2019-2.1.7-ERA-NET-2021-00021 financed by the National Research, Development and Innovation Fund of the Ministry for Innovation and Technology, Hungary. The results of this paper were presented at the 6th European Congress on Radiation Protection conference, and we thank for the support of the Hungarian Loránd Eötvös Physical Society's Health Physics Section. The research was also financed by the European Union and the State of Hungary, co-financed by the European Regional Development Fund in the project of GINOP-2.3.4-15-2020-00007.

References

[1] F.P. Glasser, International Atomic Energy Agency (IAEA), 2013, p. 30.
[2] J. Koťátková, J. Zatloukal, P. Reiterman, K. Kolář, J. Environ. Radioact. 178–179 (2017) 147.
[3] B. Batchelor, Waste Manag. 26 (2006) 689.
[4] M. Ochs, D. Mallants, L. Wang, in: Radionuclide and Metal Sorption on Cement and Concrete, Springer International Publishing, Cham, 2016, pp. 5–16.
[5] M.L.D. Gougar, B.E. Scheetz, D.M. Roy, Waste Manag. 16 (1996) 295.
[6] M. Atkins, F.P. Glasser, Waste Manag. 12 (1992) 105.
[7] P.C. Aïtcin, R. Flatt, Science and technology of concrete admixtures. 2015.
[8] D. Marchon, R.J. Flatt, in: Science and Technology of Concrete Admixtures, Publishing, Woodhead, 2016, pp. 129–145.
[9] M.M. Rusu, D. Faux, I. Ardelean, Molecules 28 (2023) 476.
[10] F. Ridi, E. Fratini, P. Baglioni, J. Colloid Interface Sci. 357 (2011) 255.
[11] F. Basquiroto de Souza, K. Sagoe-Crentsil, W. Duan, J. Am. Ceram. Soc. 105 (2022) 3081.
[12] T.C. Powers, T.L. Brownyard, J. Am. Concr. Instit. 43 (1946 to 1947) 2.
[13] R.F. Feldman, P.J. Sereda, Eng. J. 53 (1970) 53.
[14] P.J. McDonald, V. Rodin, A. Valori, Cem. Concr. Res. 40 (2010) 1656.
[15] A. Valori, in: S. University of (Ed.), University of Surrey, Guildford, 2009.
[16] A. Bede, A. Scurtu, I. Ardelean, Cem. Concr. Res. 89 (2016) 56.
[17] J.-P. Korb, L. Monteilhet, P.J. McDonald, J. Mitchell, Cem. Concr. Res. 37 (2007) 295.
[18] R. Valckenborg, L. Pel, K. Kopinga, J. Phys. D Appl. Phys. 35 (2002) 249.
[19] A.E. Osmanlioglu, Waste Manag. 22 (2002) 481.
[20] J. Ambroise, S. Maximilien, J. Pera, Adv. Cem. Bas. Mat. 1 (1994) 161.
[21] L. Mlinárik, K. Kopecskó, Mérnökgeológia-Kőzetmechanika (2011) 357.
[22] M. Nicu, L. Ionascu, C. Turcanu, F. Dragolici, G. Rotarescu, G. Dogaru, Rom. J. Phys. 53 (2008) 841.
[23] M. Kéri, A. Forgács, V. Papp, I. Bányai, P. Veres, A. Len, Z. Dudás, I. Fábián, J. Kalmár, Acta Biomater. 105 (2020) 131.
[24] M. Kéri, B. Nagy, K. László, I. Bányai, Microporous Mesoporous Mater. 317 (2021), 110988.
[25] M. Kéri, D. Nyul, K. László, L. Novák, I. Bányai, Carbon 189 (2022) 57.
[26] R. Kimmich, NMR: Tomography, Relaxometry, Springer, Berlin Heidelberg, Berlin, Heidelberg, Diffusometry, 1997, pp. 116–124.
[27] R. Kimmich, NMR Tomography, Diffusometry, Relaxometry, 2019.
[28] R.L. Kleinberg, M.A. Horsfield, J. Magn. Reson. 88 (1990) 9.
[29] P. Barrie, 2000, p. 265-316.
[30] W.P. Halperin, J.-Y. Jehng, Y.-Q. Song, Magn. Reson. Imaging 12 (1994) 169.
[31] J.P. Korb, Curr. Opin. Colloid Interface Sci. 14 (2009) 192.
[32] L. Liu, Z. He, X. Cai, S. Fu, Appl. Magn. Reson. 52 (2021) 15.
[33] A. Pop, C. Badea, I. Ardelean, Appl. Magn. Reson. 44 (2013) 1223.
[34] P.F. Faure, S. Rodts, Magn. Reson. Imaging 26 (2008) 1183.
[35] O. Petrov, I. Furo, Prog. Nucl. Magn. Reson. Spectros. 54 (2009) 97.
[36] J. Mitchell, J.B.W. Webber, J.H. Strange, Phys. Rep. 461 (2008) 1.
[37] J. Li, S. Mailhiot, H. Sreenivasan, A.M. Kantola, M. Illikainen, E. Adesanya, L. Kriskova, V.-V. Telkki, P. Kinnunen, Cem. Concr. Res. 143 (2021), 106394.
[38] M. Fleury, G. Berthe, T. Chevalier, Magn Reson Imaging 56 (2019) 32.
[39] C. J., Matematics of diffusion, second ed. Clarendon Press, Oxford, 1975.
[40] H.Y. Carr, E.M. Purcell, Phys. Rev. 94 (1954) 630.
[41] S. Meiboom, D. Gill, Rev. Sci. Instrum. 29 (1958) 688.
[42] M.D. Does, M.R. Juttukonda, R.D. Dortch, Vanderbilt University.
[43] C. Ammann, P. Meier, A. Merbach, J. Magn. Reson. 46 (1982) (1969) 319.

[44] N. Shiferaw, L. Habte, T. Thenepalli, J.-W. Ahn, Materials 12 (2019) 2483.
[45] J.-W. Lee, Y.-I. Jang, W.-S. Park, S.-W. Kim, Int. J. Concr. Struct. Mater. 10 (2016) 527.
[46] Zementwerke e.V. Verein Deutscher, Forschungsinstitut der Zementindustrie, Zement-Taschenbuch 51. Ausgabe, Verlag Bau+Technik GmbH, Düsseldorf, 2008.
[47] O. Petrov, I. Furó, PCCP 13 (2011) 16358.
[48] C. Zhou, F. Ren, Q. Zeng, L. Xiao, W. Wang, Cem. Concr. Res. 105 (2018).
[49] C. Naber, F. Kleiner, F. Becker, L. Nguyen-Tuan, C. Rößler, M.A. Etzold, J. Neubauer, Materials 13 (2020) 1779.
[50] A.C.A. Muller, K.L. Scrivener, A.M. Gajewicz, P.J. McDonald, Microporous Mesoporous Mater. 178 (2013) 99.
[51] L. Monteilhet, J.P. Korb, J. Mitchell, P.J. McDonald, Phys. Rev. E 74 (2006), 061404.
[52] S. Godefroy, J.P. Korb, M. Fleury, R.G. Bryant, Phys. Rev. E 64 (2001), 021605.
[53] M. Fleury, T. Chevalier, G. Berthe, W. Dridi, M. Adadji, Constr. Build. Mater. 259 (2020), 119843.